



OPEN

SUBJECT AREAS:
LAB-ON-A-CHIP
ATMOSPHERIC OPTICSReceived
10 January 2014Accepted
9 April 2014Published
25 April 2014Correspondence and
requests for materials
should be addressed to
Y.D. (yduan@scu.edu.
cn)

Chip-based ingroove microplasma with orthogonal signal collection: new approach for carbon-containing species detection through open air reaction for performance enhancement

Fanying Meng¹, Xuemei Li¹ & Yixiang Duan^{1,2}¹Research Center of Analytical Instrumentation, Analytical & Testing Center, Sichuan University, Chengdu, China, ²Research Center of Analytical Instrumentation, College of Life Sciences, Sichuan University, Chengdu, China.

A novel microplasma generator based on ceramic chips has been developed and coupled with optical emission spectrometry through orthogonal detection. Stable microplasma was generated between two electrodes in the ingroove discharge chamber and the optical fiber was set in perpendicular to the gas outlet to collect emitted light. The emission signal of CN is surprisingly enhanced by reacting carbon-containing species with back-diffusion nitrogen from open air, and the enhanced CN signal is successfully applied to sensitively detect organic compounds for the first time. This article focuses to study the structural characteristic and the signal enhancement mechanism through back-diffusion reaction. Several organic compounds were detected directly with the limits of detection down to ppb level. Besides, the advantages of low energy consumption and the chip-based discharge chamber show great potential to be applied in portable devices. This development may lead to a new way for the sensitive detection of organic compounds.

Due to the growing demand for real-time and in-situ sample analysis, microplasma sources have become a powerful unit in various portable devices¹. These microplasmas generally are used as excitation sources for optical emission spectrometry^{2,3}, ionization sources for mass spectrometry^{4,5} and detectors for gas chromatography^{6–8}. Although microplasma is small in size, namely at least one dimension below 1 mm, it can produce a series of highly energetic metastable particles which can provide sufficient energy to excite and ionize samples through penning ionization and energy transfer^{9,10}. Because of the unique features of small size, light weight, and low power consumption, microplasmas have great advantages in coupling with the portable and battery-operated detection systems. Furthermore, they accord with the current developing trends of modern analytical instruments: “lab on a chip”¹¹ and “micro total analysis system” (μ -TAS)^{12,13}.

Microplasmas based optical emission spectrometry are widely used to detect volatile organic compounds (VOCs)^{8,14}, inorganic gases¹⁵, and halogenated, nitrogenous, or phosphorous hydrocarbons^{16,17}. These microplasmas include glow discharge (GD)^{2,3,17}, microhollow cathode discharge (MHCD)^{18,19}, dielectric barrier discharge (DBD)²⁰, minimize microwave induced plasma (MIP)⁷, and capacitively coupled microplasma (CC μ P)^{15,21}. Glow discharge microplasmas are investigated by several laboratories because of their simple structure. Although various glow discharge microplasma detectors based optical emission spectrometry were reported in the literature^{2,3,14,22}, the previous microplasma structures are still suffering some design limitations and need to be further improved. Currently, there are two ways to collect emission light from microplasmas: an optical probe at the end of outlet^{3,17} straightly in line with plasma gas flow, and a probe that collects light through the transparent wall of the discharge chamber^{3,22}. In the first case, the carrier gas with higher flow rate is usually required to blow the microplasma out and also to ensure that the light can be effectively collected by the fiber. Carbon deposition is an issue that are brought by the incomplete combustion of organic compounds, reducing the emission light transfer to collection fiber and therefore decreases the sensitivity of detection in the second case. Furthermore, the most microplasma devices were made of glass or on fused silica wafers. The complex manufacturing progresses, such as etching micro gas channel and discharge chamber, cannot be completed manually and therefore, increasing the fabrication costs of microplasma device.



We here present a novel design of a microplasma device, namely chip-based ingroove microplasma (CIMP), with handily available ceramic plates. Stable microplasma can be easily generated between two electrodes, which were set face to face in each side of the ingroove chamber, and the optical fiber was set in perpendicular to the gas flow direction for optical signal detection. This new design not only simplified the structure of the microplasma generator, but also effectively enhanced the signals of CN species of organic compounds through the reaction between carbon-containing species and back-diffusion nitrogen from open air. Therefore, we create this way to detect various organic compounds with enhanced sensitivity. This article deals with the characteristics of the CIMP through the comparison with the microplasma jet, discusses experimentally and theoretically the signal-enhanced mechanism, optimizes the working parameters as excitation source for optical emission spectrometry, and evaluates the potential and performance of the microplasma chip for quantitative analysis by calculating the LODs, RSDs and liner correlation coefficients of calibration curves for VOCs.

Results

Microplasma chip design. Figure 1a shows the detailed schematic diagram of the ingroove microplasma on a chip. The microplasma generator (20 mm × 10 mm × 4 mm) was made on a ceramic baseboard chip (20 mm × 10 mm × 1 mm) including a gas channel, two electrodes and a discharge chamber. The gas channel and two electrodes were fixed on the ceramic baseboard chip by epoxy and ceramic bars. Besides, the discharge chamber including the groove was open to air and built by ceramic bars. Ceramic (Al_2O_3 , $\geq 99\%$) was chosen to serve as the material of microplasma generator

due to their thermo-stability, low cost and easy incision. A smooth quartz tube (1.0 mm i.d. × 2.0 mm o.d.) was used as the gas channel to reduce the fluctuation of plasma gas. The platinum electrodes were placed face to face in the ingroove discharge chamber (0.5 mm × 2 mm × 1.6 mm) and were set close to one end of the quartz tube. The gap between the two electrodes was about 0.5 mm. The length of the gas outlet was only 0.6 mm to benefit the transmission of light. The gas discharge chamber was also used as gas buffer chamber in order to keep microplasma stable and prolong the residence time of analytes in the microplasma. Based on the CIMP, a system of optical emission spectrometry was built to study the discharge mechanism and to optimize the working parameters of the CIMP as an excitation source.

The schematic diagram of the glow discharge optical emission spectrometry system is shown in figure 1b. Argon was controlled by a mass flow controller and used as discharge gas and carrier gas. The device was driven by a direct current (DC) power source. A ballast resistor was used to limit the discharge current and to prevent glow-to-arc transition. The plasma was ignited when the voltage increased to 550 V in argon. The light emitted from microplasma was picked up by the optical fiber which was perpendicular to the gas outlet of the discharge chamber. The optical emission was collected onto the entrance slit of the spectrometer. The computer was connected with the spectrometer to show spectrum and to store data. All the experiments were at room temperature and at atmospheric pressure.

Characteristics of CIMP. The ingroove microplasma was ignited when the voltage between two electrodes rose to 550 V in argon and 830 V in air. The power consumption to maintain the

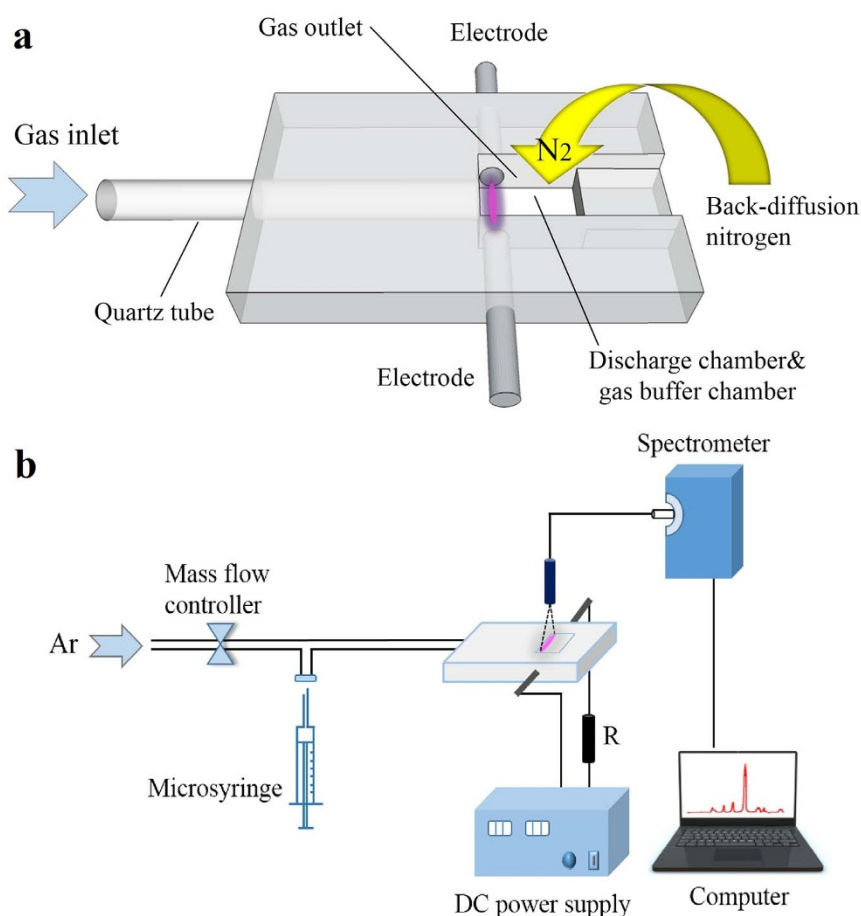


Figure 1 | Schematic diagrams of the device. (a) The schematic diagram of the ingroove microplasma on a chip. (b) The schematic diagram of the microplasma optical emission spectrometry system.

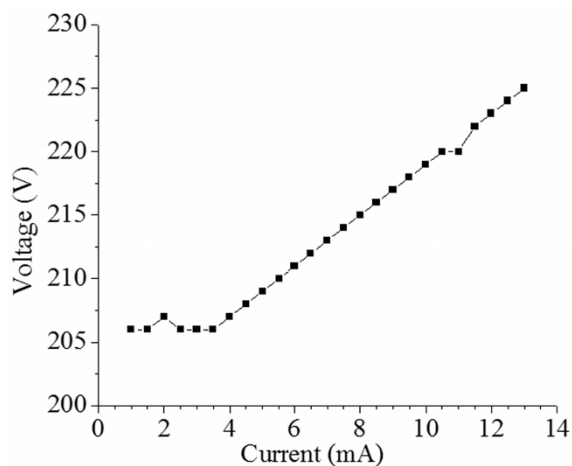


Figure 2 | Current-voltage characteristics of the microplasma device: Ar flow rate, 130 mL/min.

microplasma was only 0.1–3 W. The negative glow region and the positive column can be obviously observed from the gas outlet of discharge chamber. As shown in figure 2, the current-voltage characteristics of the microplasma were measured from 1.0 to 13 mA. The voltage remained constant as the current changed in the region of 1.0 to 3.5 mA, which is the characteristic of normal glow discharge. Under this condition, the current density at the cathode remains constant and it was found that the area of the cathode covered by the glow expanded proportionally with the increase of current^{23,24}. The cathode was fully covered when the current was beyond 3.5 mA. Then the voltage and current density were increased by increasing the current, meaning that the region was the abnormal glow discharge. The abnormal glow discharge is more commonly used to provide higher stability and detection sensitivity.

Compared with other microplasma-based excitation sources, this novel design dramatically improves the stability of microplasma and sensitivity of detection with easily available materials. Stable microplasma was easily generated and sustained between two electrodes, which was placed face to face in a cube-shaped ingroove chamber, since then the stability of microplasma was improved by avoiding the direct contact with discharge chamber and the excitation capability of this source was improved by reducing the collision of active species with the discharge chamber²⁵. Since the discharge chamber was also used as the gas buffer chamber, this design not only prolong the residence time of analytes in microplasma but also improves the stability of microplasma by reducing the fluctuation of Ar and air for discharge chamber. In addition, due to the exposure of the discharge chamber to open air, the back-diffusion nitrogen can enter into the microplasma and react with the carbon-containing species into CN species at low Ar flow rate. The emission intensity of CN species was significantly improved with this new ingroove microplasma. Therefore, the detection limits was relatively low through the analytical line of CN. This reaction mechanism will be explained in a later section. The optical fiber was perpendicular to the gas outlet of discharge chamber for detection to avoid the main effluent stream. Therefore, the fiber was not affected by any deposition and/or contamination of the effluent stream.

In order to illustrate the unique feature of this novel design of the ingroove microplasma, a comparison of this CIMP with our previous designed microplasma jet was made. The microplasma jet (Fig 3a) was used to compare its performance with the CIMP. All the parameters for the testing microplasma jet, such as its gas inlet, gap of electrodes, and breakdown voltages, were set same as CIMP. The comparison of the two types of microplasmas was made mainly in

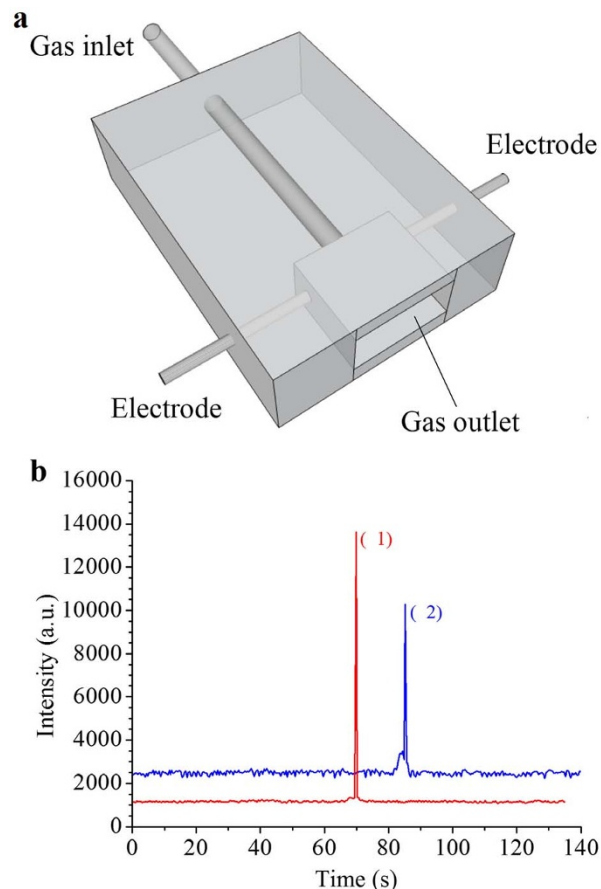


Figure 3 | (a) The schematic diagram of the microplasma jet. (b) The sequence diagram of two microplasmas at 387.20 nm in their optimized conditions: (1) CIMP: Ar flow rate, 130 mL/min; current, 10 mA; integration time, 400 ms; the number of spectrum average, 1. (2) the microplasma jet: Ar flow rate, 550 mL/min; current, 10 mA; integration time, 400 ms; the number of spectrum average, 1.

two aspects: the gas consumption, and their analytical performance for organic compounds.

The flow rate of argon for the microplasma jet was above 550 mL/min in the process of detection. Higher flow rate was required in order to blow microplasma out. However, the CIMP was not restricted with the flow rate of argon and then about 120 mL/min argon was used to reduce the disturbance of air and keep the stability of base lines for detection.

Their analytical performance for organic samples were compared by injecting 0.4 μ L acetone vapor into two microplasmas respectively in their optimized conditions. From the emission spectra (Fig. 4) of acetone with two microplasma devices, it can be observed that the emission lines of nitrogen-containing species were shown in both emission spectra, however, only the emission line of CN species was extremely strong for the CIMP. The reason for this phenomenon is that the nitrogen in the open air can be back diffusion into the core of microplasma, and react with C, CH and C₂ species and turning them into CN adequately in the CIMP. While in case of the microplasma jet, although all the emission spectra of CN, CH, and C₂ species could be observed, their intensities were relatively weak due to the higher flow rate of Ar. In such case, most nitrogen in open air can only be back diffusion into the plume of microplasma, and cannot fully react with the carbon-containing species into CN. Therefore, the CIMP is a signal-enhanced excitation source and more suitable for quantitative determination. As shown in figure 3b, the response of the CIMP for same amount of acetone was significantly higher and its base line (387.20 nm) for detection was much more stable than that of the

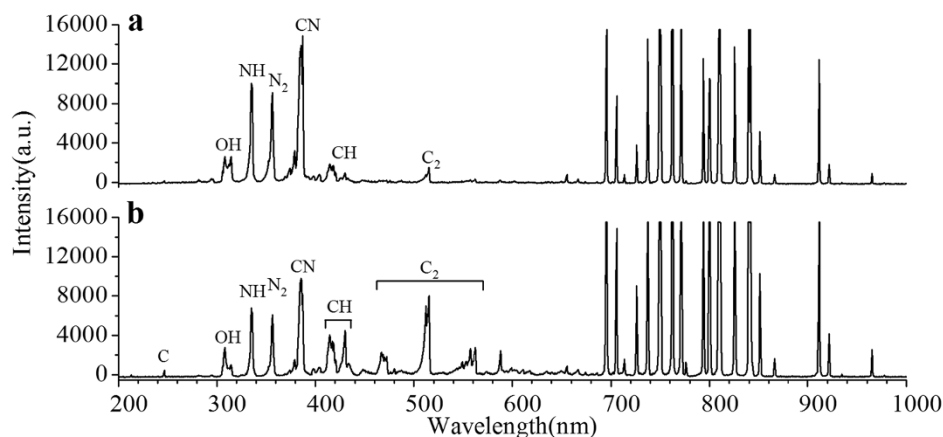


Figure 4 | The typical emission spectra. (a) The acetone spectrum with CIMP. (b) The acetone spectrum with the microplasma jet.

microplasma jet in the same integration time and the number of spectrum average of the spectrometer. The higher response and more stable base lines for organic samples indicate that the sensitivity of detection is higher than that of the microplasma jet.

Due to the lower Ar flow rate and the gas buffer chamber, the analytes can stay longer time in CIMP than that in microplasma jet. Longer residence time of CIMP contribute to the dissociation of samples and the reaction with back-diffusion nitrogen. In addition, since the microplasma in the CIMP does not interact with discharge chamber, the collision of active species with discharge chamber is reduced and more active species in microplasma can be used to excite analytes. Moreover, the microplasma is less affected by the fluctuation of Ar and air flows with the help of gas buffer chamber. This feature improves the stability of the chip-based microplasma. On the contrary, the analytes are blew out directly when they pass through the microplasma in the microplasma jet, and the higher Ar flow rate reduces the residence time of analytes in microplasma. In addition, the contact of microplasma with the gas outlet also reduces the excitation capability and the stability of microplasma jet. Therefore, the stability and sensitivity of CIMP is significantly better than that of the microplasma jet. Other organic compounds and base lines (431.43 nm and 516.03 nm) for detection were also compared between the two types of the microplasmas, and similar phenomenon was found.

Background spectra and signal enhancement mechanisms. The organic compounds were excited and ionized through two major mechanisms: Penning ionization ($M^0 + Ar^* \rightarrow M^+ + Ar^0 + e^-$), in which the potential energy of metastable argon was transferred to organic compounds resulting in excitation, and energy transfer ($M^0 + e^- \rightarrow M^+ + 2e^-$), where a kinetic energy transferred from an energetic electron to organic compounds⁹. Since metastable argon species have high excitation potentials (the 3P_2 at 11.55 eV and the 3P_0 at 11.72 eV), the samples with the ionization potential lower than metastable argon levels can be excited for providing analytical information in microplasma. Since the microplasma is a low-energy source, the samples may not be completely dissociated and their molecular spectral lines are usually used for quantitative and qualitative analysis²⁶. The background spectrum of pure Ar was shown in figure 5a, with Ar working conditions of 130 mL/min, 10 mA and 215 V. The major emission lines of argon (695.65, 762.53 nm, 771.34 nm, etc.) were gathered in the wavelengths between 690–925 nm by the transition of $4p \rightarrow 4s$. The strong emission lines of OH ($A^2\Sigma \rightarrow X^2\Pi$) at 308.81 nm, NH ($A^3\Pi \rightarrow X^3\Sigma^-$) at 335.79 nm, and N_2 ($C^3\Pi_u \rightarrow B^3\Pi_g$) at 356.66 nm and 379.81 nm were also found in the region of 280–380 nm due to the presence of impurities such as water and nitrogen in argon and back-diffusion air^{27,28}. The formation of excited N_2 and OH may

attribute to the Penning ionization ($Ar^* + N_2^0 \rightarrow N_2$ ($C^3\Pi_u$) + Ar^0 ; N_2 ($C^3\Pi_u$) \rightarrow N_2 ($B^3\Pi_g$) + $h\nu$; $Ar^* + H_2O \rightarrow OH + H + Ar^0$) and energy transfer ($N_2^0 + e^- \rightarrow N_2^* + e^-$; $H_2O + e^- \rightarrow OH + H + e^-$).

The phenomenon of back-diffusion nitrogen was mentioned in many articles before. The back-diffusion nitrogen was usually discussed as the interference of emission spectra affecting the carbon-containing species. However, we here apply the back-diffusion nitrogen to react with the carbon-containing species (C, CH and C_2) into CN and used the enhanced CN line at 387.20 nm to detect organic compounds to effectively improve the detection sensitivity. Therefore, the CN emission lines were obviously increased and the emission lines of CH and C_2 species were significantly decreased when comparing with the microplasma jet (Fig. 4). Due to the short gas outlet, nitrogen was back-diffusion into microplasma when the CIMP was ignited. The samples injected were excited into several carbon-containing species, and then these excited species reacted with back-diffusion nitrogen and therefore, emitted special lines for detection (Supplementary Fig. S1). The reaction steps of carbon-containing species with nitrogen^{29,30} probably are as follows:

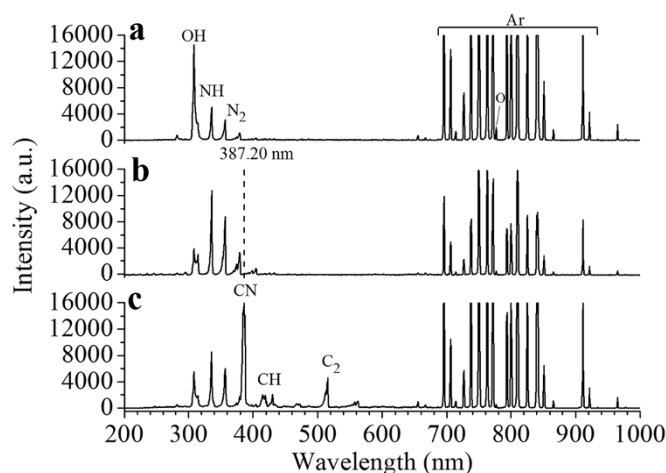
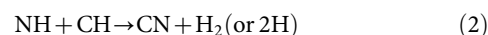
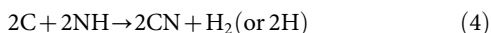


Figure 5 | The typical emission spectra: (a) pure Ar: Ar flow rate, 130 mL/min; (b) 6 μ L air was injected into microplasma: Ar flow rate, 130 mL/min; (c) 0.5 μ L saturated hexane was injected into microplasma: Ar flow rate, 130 mL/min; current: 10 mA.



From the reaction steps presented above, N_2 can react with CH , C , and C_2 species to generate CN species. For this reason, the relatively high content of N_2 in microplasma helps to improve the emission intensity of CN ($\text{B}^2\Sigma \rightarrow \text{X}^2\Sigma$). This can explain the phenomenon that the emission line of CN is strong in the emission spectra of the organic compounds which do not contain nitrogen, such as the spectra of acetone and hexane (Fig. 4a and Fig. 5c). Due to the existing of nitrogen, the emission intensity of C_2 species ($\text{a}^3\Pi_u \rightarrow \text{d}^3\Pi_g$) is decreased. However, reaction (1) and (2) are the main source of CN species, since then nitrogen reacts with CH strongly and the emission intensity of CH species ($\text{A}^2\Delta \rightarrow \text{X}^2\Pi$) is weak for CIMP. To confirm this conclusion, we experienced the effect of microplasma discharge gap (Fig. 6a) and argon flow rate (Fig. 6b) on intensities of three main emission lines to optimize detection parameter in later sections, because larger discharge gap and lower argon flow rate benefit back-diffusion nitrogen into the microplasma.

Optimization of the working parameters. Before the sample detection, the discharge gap, Ar flow rate, and discharge power were examined to achieve maximum stability and sensitivity.

The discharge gap has duple influence on detection. Larger gap may benefit the increase of the signal level, because samples can enter the gap more sufficiently to dissociate. But it also increases the breakdown voltage, according to Paschen law²³. If the gap is beyond 0.6 mm, the microplasma will be blew out and then light from microplasma will be dispersive. For this reason, the response does not increase obviously with the increase of discharge gap when the gap is beyond 0.6 mm. Four microplasma devices with different gaps were made to optimize the discharge gap, which are about 0.1 mm, 0.3 mm, 0.6 mm, and 0.9 mm, and their breakdown voltages were 230 V, 400 V, 620 V, and 860 V, respectively. These emission lines of the different microplasmas were obtained by injecting the same amount of hexane vapor at Ar flow rate of 130 mL/min (Fig. 6a) and 550 mL/min (Supplementary Fig. S2). Since larger gap brought more nitrogen from air into the microplasma, the intensity of 387.20 nm (CN , $\text{B}^2\Sigma \rightarrow \text{X}^2\Sigma$) was increased obviously with the increase of gap. Although larger gap benefits samples to enter the microplasma sufficiently, the back-diffusion nitrogen affected the intensity of C_2 considerably when the gap was beyond 0.6 mm. Therefore, the intensity of 516.20 nm (C_2 , $\text{a}^3\Pi_u \rightarrow \text{d}^3\Pi_g$) increased first and then decreased with the further increase of gap distance. The CH was affected by nitrogen all the time, and the intensity of 431.43 nm (CH , $\text{A}^2\Delta \rightarrow \text{X}^2\Pi$) was always weak in all four cases. Considering the breakdown voltage for portability of this device and detection capabilities for organic compounds, the microplasma with discharge gap 0.5 mm was used in the sample detection.

Argon was used as support gas and carrier gas in this device. Higher Ar flow rate can reduce the external disturbance to improve the stability of microplasma. But it decreases portability of this devices and inhibits molecular excitation by cooling the microplasma and discharge chamber, reducing the intensity of the excitation source, diluting the analytes and reducing the residence time of emitting species in the microplasma^{31–33}. The flow rate was optimized by repeatedly injecting the same amount of hexane vapor into CIMP with varying the argon flow rate from 40 mL/min to 730 mL/min. The emission intensities at various flow rate at 387.20 nm, 431.43 nm, and 516.05 nm were shown in figure 6b. Since back-diffusion nitrogen is decreased with the flow rate increase, the intensity at

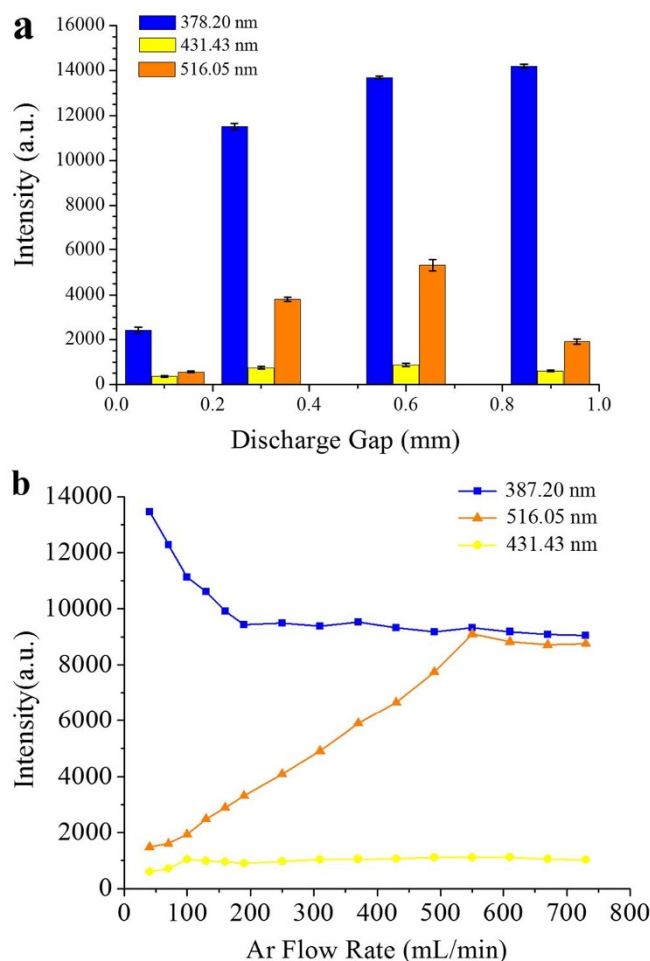


Figure 6 | Optimization of microplasma discharge gap and Ar flow rate. (a) discharge gap: Ar flow rate, 130 mL/min. (b) Ar flow rate: current, 10 mA; 0.3 μL saturated hexane.

387.20 nm (CN) firstly dropped and then remained unchanged with the further increase of flow when nitrogen tended to be balanced in microplasma. The intensity at 516.05 nm increased first and then kept constant, but always lower than the intensity at 387.20 nm.

The effect of air on analytical line at 387.20 nm was measured by injecting 6 μL air into the microplasma with argon at 130 mL/min (Fig. 5b). There was no peak at 387.20 nm in the air emission spectrum. Therefore, air has no effect on analytical line of 387.20 nm, and the carbon in CN species all comes from organic compounds. Furthermore, the nitrogen in microplasma is sufficient for trace amounts of samples. Therefore, the emission line of CN at 387.20 nm was used as analytical line of organic samples to quantitative analysis. Since the baseline was less stable when the argon flow rate was below 120 mL/min, the flow rate of 120 ~ 130 mL/min was used for sample detection³⁴. This rate range can greatly reduce the consumption of gas, and improve the response of CN (387.20 nm) through the increase of back-diffusion nitrogen, as well as ensure the stability of the microplasma. The typical emission spectrum of hexane in the optimized Ar flow rate was shown in figure 5c.

The discharge power in detection is also a major factor which determines the operational characteristics of the microplasma source. In the progress of optimization of power, the increase of discharge current was beneficial for the emission intensity. However, the emission intensity tended to remain constant, when the current was more than 10 mA (Supplementary Fig. S3). So the discharge current of 10 mA and power of 2.15 W were used to detect organic samples in the following experiments.



Table 1 | Analytical performance of CIMP with direct injection

Compound	LOD (pg)	LOD (ppb v/v)	R ²
Acetone	80	3.4	0.997
Pentane	75	3.9	0.992
Hexane	104	3.2	0.998
Methanol	115	3.6	0.999
Ether	55	2.6	0.996
Benzene	135	3.1	0.992

Analytical performance. To evaluate the analytical potential of this CIMP as the excitation source of optical emission spectrometry, several common VOCs were detected, including acetone, hydrocarbons, methanol, ether, and benzenes. All the detection processes were done in optimized conditions and the emission line of CN at 387.20 nm was measured and calibrated. Linear correlation coefficients of calibration curves for these analytes were all better than 0.99, which can be further improved through automatic injection system. The calibration curve of hexane was shown in Supplementary Figure S4 and a limit of detection (LOD) of 3.2 ppb (104 pg) for hexane was obtained. The LODs of several other compounds were in a few ppb (v/v) as shown in table 1. The precision, expressed as relative standard deviations (RSDs) of 11 replicate measurements, was 1.8% ~ 4.1% (Supplementary Fig. S5).

Generally, carbon deposition and short lifetime of the electrodes are the main limitations of direct current microplasma³. However, in this work, little carbon deposition was found in the discharge chamber for CIMP and therefore, had no effect on the emission intensity of microplasma. One important reason for little carbon deposition is that nitrogen and oxygen in the back-diffusion air can reduce carbon deposition inside the discharge chamber. Platinum with low sputtering was used as electrodes and prolonged the lifetime of the microplasma. The performance of this device had no obvious change during several months running.

Discussion

A novel chip-based ingroove microplasma (CIMP) was successfully used as an excitation source for optical emission spectrometer. Experiments have been demonstrated that the design of CIMP can effectively improve the stability of microplasma and enhance the signal of the analytical line CN. The enhanced emission line of CN at 387.20 nm was applied to detect organic compounds. The LODs of organic compounds were down to several ppb (v/v) and linear correlation coefficients of calibration curves were better than 0.99. Therefore it is sensitive and accurate for the detection of organic samples. The structure of the source will be further optimized to improve the system performance and the new source will be integrated and assembled into a portable optical spectrometer for total organic carbon detection, or coupled to a gas chromatography for separation and detection of the mixture of organic compounds in the future. More importantly, the features of low gas consumption, low power consumption, small size, easy operation, good sensitivity and good reproducibility show great potentials for this new source in practical use. The CIMP could be applied for field-portable and real-time detection, such as the air quality monitoring of factories and residential areas.

Methods

Chemicals and reagents. All chemicals were of analytical-reagent grade and used directly without any further purification. Argon (99.99%) provided by Qiao Yuan Gas Company (Chengdu, China) was used as both carrier gas and support gas.

System and procedures in detail. Argon was used as discharge gas and carrier gas. Gas flow rate was controlled by a mass flow controller (D07-19B, Sevenstar, Beijing, China) in the range of 0–1000 mL/min. The device was driven by a direct current power source (Dongwen Corporation, Tianjin, China). A 50 k Ω ballast resistor was used to limit the discharge current and to prevent glow-to-arc transition. The plasma

was ignited when the voltage increased to 550 V in argon. The light emitted from microplasma was picked up by the optical fiber which was set in perpendicular to the gas outlet of the discharge chamber. The optical emission was collected onto the entrance slit of the spectrometer (HR2000+, Ocean Optics Inc., FL, USA.). This linear CCD-array detector with 2048-element pixels was able to detect the whole spectrum from 200 to 1100 nm. The computer was connected with the spectrometer to show spectrum and to store data.

Safety hazard note. The CIMP calls for DC voltage up to several hundred volts to generate the microplasma, thus care should be taken in order to avoid electric shot.

Calculation of microplasma power. The microplasma power was calculated as the current of the discharge circuit multiplies the voltage between the two electrodes. The voltage between the two electrodes obtained by the voltage of the discharge circuit subtracts the voltage of the ballast resistor.

Sample introduction. The organic samples were introduced with a microsyringe by manual injection from the gas inlet line to evaluate the potential of this microplasma chip for quantitative analysis. These VOCs were diluted with argon in gas sampling bags. A certain amount of liquid of highly VOCs, such as hexane and acetone, were respectively injected into the 0.5 L aluminum foil bags which were filled with a known volume of argon before. The bags were kept at room temperature for hours to ensure the liquid volatilized completely. Then several-microliter gases were injected directly into inlet line with argon for detection.

Calculation of limits of detection. The limits of detection (LODs) were calculated as $3 s m^{-1}$, where s was the standard deviation of 11 blank measurements and m was the slope of the calibration curve, respectively.

- Karanassios, V. Microplasmas for chemical analysis: analytical tools or research toys? *Spectrochim. Acta, Part B* **59**, 909–928 (2004).
- Jin, Z., Su, Y. & Duan, Y. A low-power, atmospheric pressure, pulsed plasma source for molecular emission spectrometry. *Anal. Chem.* **73**, 360–365 (2001).
- Eijkel Jan, C. T., Stoeri, H. & Manz, A. A molecular emission detector on a chip employing a direct current microplasma. *Anal. Chem.* **71**, 2600–2606 (1999).
- Ding, X., Zhan, X., Yuan, X., Zhao, Z. & Duan, Y. Microfabricated glow discharge plasma (mfgdp) for ambient desorption/ionization mass spectrometry. *Anal. Chem.* **85**, 9013–9020 (2013).
- Symonds, J. M., Galhena, A. S., Fernández, F. M. & Orlando, T. M. Microplasma discharge ionization source for ambient mass spectrometry. *Anal. Chem.* **82**, 621–627 (2010).
- Duan, Y., Su, Y. & Jin, Z. Capillary-discharge-based portable detector for chemical vapor monitoring. *Rev. Sci. Instrum.* **74**, 2811–2816 (2003).
- Hoskinson, A. R., Hopwood, J., Bostrom, N. W., Crank, J. A. & Harrison, C. Low-power microwave-generated helium microplasma for molecular and atomic spectrometry. *J. Anal. At. Spectrom.* **26**, 1258–1264 (2011).
- Fu, Y.-M., Chu, S.-C. & Lu, C.-J. Characteristic responses of an atmospheric pressure DC micro-plasma detector for gas chromatography to organic functional groups. *Microchem. J.* **89**, 7–12 (2008).
- Smith, R. L., Serxner, D. & Hess, K. R. Assessment of the relative role of penning ionization in low-pressure glow discharges. *Anal. Chem.* **61**, 1103–1108 (1989).
- Becker, K. H., Schoenbach, K. H. & Eden, J. G. Microplasmas and applications. *J. Phys. D: Appl. Phys.* **39**, R55–R70 (2006).
- Luo, D. & Duan, Y. Microplasmas for analytical applications of lab-on-a-chip. *TrAC* **39**, 254–266 (2012).
- Manz, A., Graber, N. & Widmer, H. M. Miniaturized total chemical analysis systems: a novel concept for chemical sensing. *Sens. Actuators, B* **1**, 244–248 (1990).
- Auroux, P., Iossifidis, D., Reyes, D. & Manz, A. Micro total analysis systems. 2. analytical standard operations and applications. *Anal. Chem.* **74**, 2637–2652 (2002).
- Yuan, X., Ding, X., Zhao, Z., Zhan, X. & Duan, Y. Performance evaluation of a newly designed DC microplasma for direct organic compound detection through molecular emission spectrometry. *J. Anal. At. Spectrom.* **27**, 2094–2101 (2012).
- Guchardi, R. & Hauser, P. C. Capacitively coupled microplasma for on-column detection of chromatographically separated inorganic gases by optical emission spectrometry. *J. Chromatogr. A* **1033**, 333–338 (2004).
- Guchardi, R. & Hauser, P. C. Determination of non-metals in organic compounds by gas chromatography with a miniature capacitively coupled plasma emission detector. *J. Anal. At. Spectrom.* **19**, 945–949 (2004).
- Liu, Y., Cao, W., Ding, X., Yuan, X. & Duan, Y. Characterization of the analytical capabilities of an atmospheric micro-plasma device for the detection of nonmetals. *Spectrochim. Acta, Part B* **76**, 152–158 (2012).
- Meyer, C. et al. Development of a novel dielectric barrier microhollow cathode discharge for gaseous atomic emission spectroscopy. *J. Anal. At. Spectrom.* **27**, 677–681 (2012).
- Quan, X., Chen, S., Platzer, B., Chen, J. & Gfrerer, M. Simultaneous determination of chlorinated organic compounds from environmental samples using gas chromatography coupled with a micro electron capture detector and micro-plasma atomic emission detector. *Spectrochim. Acta, Part B* **57**, 189–199 (2002).



20. Li, W. *et al.* Dielectric barrier discharge molecular emission spectrometer as multichannel GC detector for halohydrocarbons. *Anal. Chem.* **83**, 5050–5055 (2011).
21. Guchardi, R. & Hauser, P. C. A capacitively coupled microplasma in a fused silica capillary. *J. Anal. At. Spectrom.* **18**, 1056–1059 (2003).
22. Tienpont, B. *et al.* Features of a micro-gas chromatograph equipped with enrichment device and microchip plasma emission detection (μ PED) for air monitoring. *Lab Chip* **8**, 1819–1828 (2008).
23. Roberto, M., Smith, H. B. & Verboncoeur, J. P. Influence of metastable atoms in radio-frequency argon discharges. *IEEE Trans. Plasma Sci.* **31**, 1292–1298 (2003).
24. Raizer, Y. P. Stable glow discharge. *Gas Discharge Physics*. Allen, J. E. (ed.), 167–213. Springer-Verlag, Berlin, 1991.
25. Boumans, P. W. J. M. Studies of sputtering in a glow discharge for spectrochemical analysis. *Anal. Chem.* **44**, 1219–1228 (1972).
26. Harrison, W. W. Glow discharge: considerations as a versatile analytical source. *J. Anal. At. Spectrom.* **7**, 75–79 (1992).
27. Patel, B. M., Heithmar, E. & Winefordner, J. D. Tubular electrode torch for capacitively coupled helium microwave plasma as a spectrochemical excitation source. *Anal. Chem.* **59**, 2374–2377 (1987).
28. Peter, S. A., Uden, P. C. & Barnes, R. M. Microwave-excited atmospheric pressure helium plasma emission detection characteristics in fused silica capillary gas chromatography. *Anal. Chem.* **53**, 1829–1837 (1981).
29. Braman, R. S. & Dynako, A. Direct current discharge spectral emission-type detector. *Anal. Chem.* **40**, 95–106 (1968).
30. Vivien, C., Hermann, J., Perrone, A., Boulmer-Leborgne, C. & Luches, A. A study of molecule of formation during laser ablation of graphite in low-pressure nitrogen. *J. Phys. D: Appl. Phys.* **31**, 1263–1272 (1998).
31. Estes, S. A., Uden, P. C. & Barnes, R. M. Microwave-excited atmospheric pressure helium plasma emission detection characteristics in fused silica capillary gas chromatography. *Anal. Chem.* **53**, 1829–1837 (1981).
32. Quimby, B. D. & Sullivan, J. J. Evaluation of a microwave cavity, discharge tube, and gas flow system for combined gas chromatography-atomic emission detection. *Anal. Chem.* **62**, 1027–1034 (1990).
33. Skelton, R. J., Markides, K. E., Lee, M. L. & Farnsworth, P. B. Characterization of near-infrared atomic emission from a radio-frequency plasma for selective detection in capillary gas chromatography. *Appl. Spectrosc.* **44**, 853–857 (1990).
34. Quimby, B. D., Uden, P. C. & Barnes, R. M. Atmospheric pressure helium microwave detection system for gas chromatography. *Anal. Chem.* **50**, 2112–2118 (1978).

Acknowledgments

The authors are grateful to the financial support from National Recruitment Program of Global Experts (NRPGE), the Hundred Talents Program of Sichuan Province (HTPSP), and the Startup Funding of Sichuan University for setting up the Research Center of Analytical Instrumentation.

Author contributions

X.L., F.M. and Y.D. conceived the original idea. F.M. designed and executed the experiment under the guidance of Y. D. Finally, F. M., X. L. and Y. D. analyzed the results and wrote the paper.

Additional information

Supplementary information accompanies this paper at <http://www.nature.com/scientificreports>

Competing financial interests: The authors declare no competing financial interests.

How to cite this article: Meng, F.Y., Li, X.M. & Duan, Y.X. Chip-based ingroove microplasma with orthogonal signal collection: new approach for carbon-containing species detection through open air reaction for performance enhancement. *Sci. Rep.* **4**, 4803; DOI:10.1038/srep04803 (2014).



This work is licensed under a Creative Commons Attribution-NonCommercial-NoDerivs 3.0 Unported License. The images in this article are included in the article's Creative Commons license, unless indicated otherwise in the image credit; if the image is not included under the Creative Commons license, users will need to obtain permission from the license holder in order to reproduce the image. To view a copy of this license, visit <http://creativecommons.org/licenses/by-nc-nd/3.0/>